Molecular Communication in Fractional Diffusive Channel

Author 1, Author 2, and Author 3

***Abstract*—The molecular communication system with anomalous/fractional diffusion inside a one-dimensional (1-D) environment is considered. The time-dependent diffusivity is incorporated in terms of the power-law diffusivity, and the expression of first passage time density (FPTD) is derived. Further, the peak pulse time and peak concentration corresponding to the derived FPTD function are obtained. Moreover, the analysis is extended in terms of the average probability of error and throughput for the anomalous diffusion channel. The analytical results are validated through simulations.**

***Index Terms*—Anomalous diffusion, fractional diffusion equation, molecular communication and throughput.**

I. Introduction

Molecular communication (MolCom) is an evolving communication technology, where the molecules are used as an information carrier to exchange the information between the transmitter (TX) and receiver (RX) [1]. In the available MolCom literature, the most widely used channel for study is the diffusive channel, i.e., the displacement of particles occurs solely due to Brownian motion [2]. In the simplest case of diffusion, the mean square displacement (MSD) of a particle in Brownian motion scales linearly with time. For this reason many works in MolCom have considered diffusive channels where the MSD of particles varies linearly with time. However, this linear dependence is not true in general, and in certain applications the MSD of particles varies non-linearly with time and in these cases the motion of a particle is known as non-Brownian motion. In such diffusion processes, the MSD is considered to scale as a fractional exponent of time, and the processes are known as fractional diffusion processes [3].

The anomalous/fractional diffusion is observed in numerous spatially disordered systems such as in plasmas and turbulent fluids, and in biological media with traps, receptor binding sites or macro-molecular crowding [4]. Extensive literature on anomalous diffusion can be found in [5], [6] and references therein, where various models and analytical methods have been proposed to describe the mechanisms of anomalous diffusion. The analytical modeling of anomalous diffusion is generally classified in one of four ways [5]: (i) fractional Brownian motion (fBm), (ii) scaled Brownian motion (SBM), (iii) Levy flight, (iv) continuous-time-random-walk (CTRW). The first two classes follow a Gaussian model, whereas the latter two classes fall into the category of non-Gaussian models [6]. In CTRW, a tagged particle waits for a random time-step between two consecutive jumps. The CTRW can be Markovian or non-Markovian, as determined by the waiting time distribtuion (WTD). For example, exponential WTD corresponds to the Markovian CTRW, whereas any non-exponential WTD corresponds to a non-Markovian CTRW. Moreover, the CTRW is always a non-Gaussian process. However, an SBM is always a Gaussian process and holds the non-Markovian property due to the power-law time dependent diffusion coefficient [7]. Further details of each model can be found in [5]–[7] and references therein.

In a fractional diffusive medium, the analysis of MolCom is a challenging task. Recently, several works in the literature, including [8]–[12], have analyzed the fractional diffusive channel in MolCom systems. The first-passage-time-density (FPTD) function for the fractional diffusive medium has been obtained in [8] using the Caputo fractional derivative and the channel has been analyzed in terms of bit error rate. In [9], the authors considered the super-diffusive channel as a special case of fractional diffusion and provided a technique for optimum detection at the RX. An online event detection method which can cope with fractional diffusion without knowing the statistical knowledge of channel conditions was proposed in [10]. The stochasticity of an anomalous diffusive channel is analyzed in [11]. Recently, authors in [12] used H-diffusion modeling to analyze the anomalous diffusion phenomenon in MolCom with a timing modulation method.

We note that in [8], [11], [12], authors have used the generalized space-time fractional diffusion equation with a composite fractional time derivative that involves the H-function. In [9], sub-diffusive behavior was only analyzed with the CTRW model. However, handling the Fox's H-function is analytically complex when compared to the SBM model[1], which uses a Gaussian distribution for the spatiotemporal distribution of particles. The analysis of a fractional diffusive channel using an SBM model is computationally less complex and analytically tractable, yet is still an open problem in the MolCom literature. Moreover, the pulse peak time and pulse peak response are important metrics for analyzing MolCom channels. The analytical study of these metrics is also yet to be done for an anomalously-diffusive channel. Furthermore, in [14], [15] and references therein, the error probability and information rate have been analyzed for the normally diffusive channel, however these metrics for an anomalously-diffusive channel are still unexplored. Based on these motivations, our main contributions in this paper are as follows:

1) We consider the anomalous diffusion phenomenon for molecule propagation inside a 1-D fractional diffusive channel[2], and the FPTD is derived con-

[1]The water diffusion in brain tissue as measured by MRI can be analyticaly modeled using the SBM model [13].

[2]The MolCom channel can be approximated as a 1-D channel when the length of channel is much greater than its height, such that the molecules diffuse more along x-axis than y-axis [16]. Such approximations are valid in several MolCom applications such as lab-on-chip [17] and nanoporous flow systems [18].

sidering the power-law diffusivity. Further, the expression for cumulative density function (CDF) of hitting probability of molecules is also derived.
2) The expressions for pulse peak time corresponding to the spatiotemporal probability density function (PDF) of molecules, and FPTD are obtained. Furthermore, the corresponding pulse peaks are derived.
3) Using the optimal detector developed for normal diffusion in [14], [15], the anomalously-diffusive communication channel is analyzed in terms of average probability of error and throughput.

The derived analytical expressions are verified using Monte-Carlo and particle-based simulation approaches.

II. Fractional Diffusion Channel Model

The anomalous diffusion of molecules is mathematically governed by a fractional diffusion equation. One of the simplest ways to define anomalous diffusion is using time-dependent diffusivity in which the instantaneous diffusion coefficient $D(t)$ of molecules is time-varying and depends on effective diffusion coefficient (D_f) as [6]

$$D(t) = \alpha t^{\alpha-1} D_f, \tag{1}$$

where α is the anomalous diffusion exponent and ranges over $0 \leq \alpha \leq 2$. The parameter α defines three types of diffusion phenomena, **a)** normal diffusion ($\alpha = 1$) corresponds to ordinary Brownian motion, and **b)** sub-diffusion ($\alpha \leq 1$), and **c)** super-diffusion ($\alpha \geq 1$) correspond to the SBM [6]. The impulsive release of the molecules is considered at a point x_o and time t_o, which satisfies the initial conditions $c(x, t = t_o|x_o) = \delta(x = x_o)$, where $c(x, t)$ denotes the PDF of spatiotemporal distribution of molecules, and δ denotes an impulse function. Let us consider x_a is a perfectly absorbing point along the x-axis, and imposes the boundary condition $c(x = x_a, t) = 0$, i.e., the tagged molecule is completely absorbed upon reaching x_a. For the given initial conditions, according to Fick's second law of diffusion the evaluation of concentration for particles with SBM in a 1-D medium is given by [3, eq. (1.66)] as

$$\frac{\partial c(x, t|x_o)}{\partial t} = \alpha t^{\alpha-1} D_f \frac{\partial^2 c(x, t|x_o)}{\partial x^2}. \tag{2}$$

Note that the above equation is also known as effective Fokker-Planck equation for SBM. When $x_a \to \infty$, i.e., without the absorbing point in the medium, the solution of (2) can be obtained as

$$c(x, t|x_o) = \frac{1}{\sqrt{4\pi D_f t^{\alpha}}} \exp\left(-\frac{(x - x_o)^2}{4 D_f t^{\alpha}}\right). \tag{3}$$

Remark: It can be observed that the PDF shown in (3) follows the standard Gaussian distribution with variance $\sigma_m^2 = 2D_f t^{\alpha}$, and is non-Markovian due to the power law diffusivity [7]. Moreover, the MSD of particles is equal to σ_m^2 i.e., $\langle x^2 \rangle \sim 2D_f t^{\alpha} = 2D_f t^{2H}$, where H denotes the Hurst exponent and $0 \leq H \leq 1$ [5]. In anomalous diffusion, the Hurst exponent related to α as $H = \frac{\alpha}{2}$, is an important parameter in SBM and fBm, as it defines the different types of anomalous diffusion as $0 < H < 1/2$, $H = 1/2$, and $1/2 < H < 1$, corresponding to sub-diffusion, normal diffusion, and super-diffusion, respectively [5].

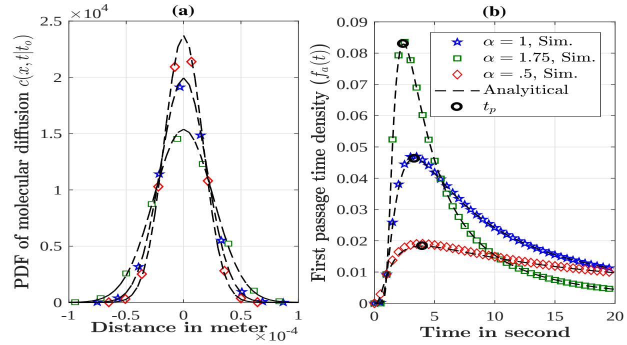

Fig. 1: Effect of anomalous diffusion on, (a) the PDF of spatiotemporal concentration, for the parameters: $D_f = 100\,\mu\text{m}^2$/s, and $t = 2$ s, and (b) FPTD function of molecules for the parameters: $D_f = 5\,\mu\text{m}^2$/s, and $x_a = 10\,\mu$m.

Lemma 1. *The FPTD for a tagged molecule arrival at the point x_a originating from the point x_o in a 1-D anomalous diffusive environmental is derived as*

$$f_p(t) = \frac{|x_a - x_o|}{\sqrt{4\pi D_f t^{\alpha+2}}} \exp\left(\frac{-(x_a - x_o)^2}{4 D_f t^{\alpha}}\right). \tag{4}$$

Proof. The proof is given in Appendix-A. □

Fig. 1 shows the PDF given in (3) and FPTD derived in Lemma 1 which describes and compares the characteristics of three types of diffusion phenomena: normal diffusion ($\alpha = 1$), sub-diffusion ($\alpha \leq 1$) and super-diffusion ($\alpha \geq 1$). In Fig. 1(a), it is assumed that there is no absorbing point in the channel. The Monte-Carlo simulations are performed for 10^5 realizations. In this figure, it can be observed that the spatiotemporal concentration for sub-diffusion phenomenon has a light-tailed distribution when compared to the other two diffusions, on the other hand super-diffusion has a heavy-tailed distribution. In other words, higher α leads to a larger MSD.

Fig. 1(b) shows the FPTD function derived in (4) and verified using particle-based simulations (PBS) for 10^4 realizations. For PBS the total time-interval is chosen as 20 s and the location of each molecule is traced in small time-steps $\Delta t = 0.1$ s until it reaches the absorbing point. The displacement of a single molecule follows the normal distribution $\Delta x \sim \mathcal{N}(0, \sigma_m^2)$, where $\sigma_m^2 = 2D_f(\Delta t)^{\alpha}$ [3]. From Fig. 1(b) it can be observed that for sub-diffusion, the FPTD function is more dispersed due to its lower mean square displacement compared to the other two diffusion phenomena. Moreover, the super-diffusion achieves a higher PDF peak faster when compared to the other two diffusion phenomena due to a higher MSD.

Lemma 2. *The pulse peak time corresponding to the*

FPTD function and spatiotemporal PDF are obtained as

$$t_{p,1} = \left(\frac{\alpha d^2}{2D_f(\alpha+2)}\right)^{\frac{1}{\alpha}}, \quad \textit{and} \quad t_{p,2} = \left(\frac{d^2}{2D_f}\right)^{\frac{1}{\alpha}}, \quad (5)$$

respectively, where d is the distance between the release and absorbing points of a molecule, and the corresponding peak values are

$$f_p(t_{p,1}) = \sqrt{\frac{\alpha+2}{2\pi\alpha}}\left(\frac{2D_f(\alpha+2)}{d^2\alpha}\right)^{\frac{1}{\alpha}}\exp\left(\frac{-(\alpha+2)}{2\alpha}\right), \quad (6)$$

$$\textit{and} \quad c_p(t_{p,2}) = \frac{1}{d\sqrt{2\pi e}}, \quad (7)$$

respectively.

Proof. The pulse peak time of the FPTD function is obtained by differentiating (4) with respect to the variable t and equating it to zero, i.e., $\frac{\partial f_p(t)}{\partial t} = 0$. We get

$$\exp\left(\frac{-d^2}{4D_f t^\alpha}\right)\frac{d}{t\sqrt{4\pi D_f t^\alpha}}\left[\frac{\alpha d^2}{4D_f t^\alpha} - \frac{(\alpha+2)}{2}\right] = 0. \quad (8)$$

After some mathematical simplifications of (8), the pulse peak time $t_{p,1}$ results in (5) and after substituting the value of $t_{p,1}$ into (4) the peak response is obtained as (6). For the normal diffusion case ($\alpha = 1$), the pulse peak time $t_{p,1} = d^2/6D_f$. The peak time $t_{p,1}$ and corresponding peak $f_p(t_{p,1}1)$ is shown in Fig. 1(b) using the black circle ('$\circ$') marker which closely matches with the simulations.

To obtain the peak pulse time corresponding to the spatiotemporal PDF ($c(x, t, x_o)$), we differentiate (3) and equate it to zero, resulting in (5). Note that for $\alpha = 1$ (normal diffusion) the pulse peak time is $t_{p,2} = \frac{d^2}{2D_f}$, which is the same as that given in [19]. □

III. Communication Channel Model

A TX and a RX positioned at x_o and x_a, respectively, are considered in the 1-D anomalous diffusive medium. The TX transmits binary information towards the RX using information-carrying molecules having instantaneous diffusion coefficient $D(t)$ as given in (1). The communication channel between the nanomachines is divided into K time-slots i.e., binary sequence $\mathrm{B}_1^K = \{b[1], b[2], \ldots, b[K]\}$ is transmitted in K time-slots, where $b[j]$ denote the symbol transmitted in the jth time-slot and $j \in \{1, 2, \ldots K\}$. The jth time-slot is defined as the time period $[(j-1)\tau, j\tau]$, where τ is the duration of one slot. For transmission of binary information, on-off-keying (OOK) method is used. In OOK at the beginning of each time-slot, the TX emits Q_s number of molecules with prior probability β_1 for transmission of information symbol '1' or remains silent for transmission of information symbol '0' with prior probability β_0. Let the binary sequence $\widehat{\mathrm{B}}_1^K = \{\widehat{b}[1], \widehat{b}[2], \ldots, \widehat{b}[K]\}$ denote the received information at RX, where $\widehat{b}[j]$ denotes the jth received bit corresponding to the transmitted bit $b[j]$. For the mathematical ease and in line with the assumptions in [20], the nanomachines are considered to be perfectly synchronized. The molecules emitted from TX follow 1-D anomalous diffusion and reach the RX at random times. Further, we assume that the motion of each particle is independent and also they independently reach the RX. Let p_{j-i} denote the probability that molecules are transmitted in ith time-slot from TX and arrive in the jth time-slot at RX. The probability p_{j-i} can be obtained using the FPTD $f_p(t)$ derived in (4) as $p_{j-i} = \int_{(j-i)\tau}^{(j-i+1)\tau} f_p(t)dt = [F(j-i+1)\tau - F(j-i)\tau]$, where $F(t)$ is the CDF derived in Lemma 1.

IV. Performance Analysis of Anomalous Diffusive Communication Channel

The number of molecules received at the receiver in the jth time-slot that were transmitted in the ith time-slot follows a Binomial distribution. For a large number of transmitted molecules and low arrival probability, the total number of received molecules is approximated as a Poisson-distributed random variable (r.v.). Let $N[j]$ be the *total* number of molecules received at RX in the jth time-slot, which as a sum of Poisson random variables is also a Poisson r.v. i.e., $N[j] \sim \mathcal{P}\left(\lambda_{b[j]}[j]\right)$, $b[j] \in \{0, 1\}$, where, $\lambda_{b[j]}[j] = b[j]Q_s p_0 + \sum_{i=1}^{j-1} b[j-i]Q_s p_i$ is the total expected number of molecules at RX for the transmitted bit $b[j]$. Here, the first and second terms are expected number of intended and inter-symbol-interference (ISI) molecules, respectively. The terms p_0 and p_i denote the arrival probabilities of molecules in the intended and interfering time-slots, respectively. Based on the number of molecules received at RX, the decision rule corresponding to the optimal decision threshold $\eta^*[j]$ is defined as[3]

$$\widehat{b}[j] = \begin{cases} 1, & \text{if } N[j] \geq \eta^*[j], \\ 0, & \text{otherwise.} \end{cases} \quad (9)$$

1) Average Probability of Error: Without prior knowledge of symbol transmission, the expression for probability of error for OOK, in the jth time-slot, for given possible ISI sequence B_1^{j-1} is obtained as [14], [15]

$$\begin{aligned} P_e[j|\mathrm{B}_1^{j-1}] &= \Pr(\widehat{b}[j] = 0|b[j] = 1, \mathrm{B}_1^{j-1})\Pr(b[j] = 1) \\ &+ \Pr(\widehat{b}[j] = 1|b[j] = 0, \mathrm{B}_1^{j-1})\Pr(b[j] = 0), \quad (10) \end{aligned}$$

where the terms $\Pr(\widehat{b}[j] = 0|b[j] = 1, \mathrm{B}_1^{j-1})$ and $\Pr(\widehat{b}[j] = 1|b[j] = 0, \mathrm{B}_1^{j-1})$ are defined as

$$\Pr(\widehat{b}[j] = 0|b[j] = 1, \mathrm{B}_1^{j-1}) = \sum_{l=1}^{\lfloor \eta[j] \rfloor} \frac{e^{-\lambda_1[j]}(\lambda_1[j])^l}{l!},$$

$$\Pr(\widehat{b}[j] = 1|b[j] = 0, \mathrm{B}_1^{j-1}) = 1 - \sum_{l=1}^{\lfloor \eta[j] \rfloor} \frac{e^{-\lambda_0[j]}(\lambda_0[j])^l}{l!},$$

[3] The expression for optimal threshold $\eta^*[j]$ which optimizes the system error performance was derived in [14] as $\eta^*[j] = \frac{\ln(\beta_0/\beta_1) + Q_s p_0}{\ln(\lambda_1[j]) - \ln(\lambda_0[j])}$. We note that the value of $\eta^*[j]$ depends on the value of p_{j-i}, which depends on the value of anomalous diffusion exponent α. Thus, anomalous diffusion affects the value of $\eta^*[j]$.

where $\lfloor \Phi \rfloor$ gives the largest integer less than or equal to Φ, and η is an arbitrary decision threshold. The end-to-end average probability of error in the jth time-slot, $\overline{P}_e[j]$, is obtained by averaging $P_e[j|\mathrm{B}_1^{j-1}]$ over all possible realizations of B_1^{j-1}, i.e., $\overline{P}_e[j] = \sum_{\mathrm{B}_1^{j-1} \in \chi} \Pr(\mathrm{B}_1^{j-1}) P_e[j|\mathrm{B}_1^{j-1}]$, where χ is the set of all possible realizations of B_1^{j-1}, and $\Pr(\mathrm{B}_1^{j-1})$ is the probability of occurrence of B_1^{j-1}.

2) Throughput: Let $b[j]$ and $\widehat{b}[j]$ be two discrete random variables that represent the transmitted and received symbols in the jth time-slot, respectively. The conditional mutual information in the jth time-slot between $b[j]$ and $\widehat{b}[j]$ can be obtained as

$$I(b[j]; \widehat{b}[j]|\mathrm{B}_1^{j-1}) = \sum_{b[j] \in \{0,1\}} \sum_{\widehat{b}[j] \in \{0,1\}} \Pr(\widehat{b}[j]|b[j], \mathrm{B}_1^{j-1}) \times \Pr(b[j]|\mathrm{B}_1^{j-1}) \log_2 \frac{\Pr(\widehat{b}[j]|b[j], \mathrm{B}_1^{j-1})}{\Pr(\widehat{b}[j]|\mathrm{B}_1^{j-1})}, \tag{11}$$

where

$$\begin{aligned}\Pr(\widehat{b}[j] = 0|\mathrm{B}_1^{j-1}) &= \Pr(\widehat{b}[j] = 0|b[j] = 0, \mathrm{B}_1^{j-1})\beta_0 \\ &+ \Pr(\widehat{b}[j] = 0|b[j] = 1, \mathrm{B}_1^{j-1})\beta_1 \\ &= (1 - P_f[j|\mathrm{B}_1^{j-1})])\beta_0 + (1 - P_d[j|\mathrm{B}_1^{j-1})])\beta_1,\end{aligned}$$

and, $\Pr(\widehat{b}[j] = 1|\mathrm{B}_1^{j-1}) = P_f[j|\mathrm{B}_1^{j-1})]\beta_0 + P_d[j|\mathrm{B}_1^{j-1})]\beta_1$, here $P_f[\cdot] = \Pr(\widehat{b} = 1|b = 0)$, and $P_d[\cdot] = \Pr(\widehat{b} = 1|b = 1)$, denote the probability of false alarm and probability of detection, respectively. Now the maximum mutual information $(I_m^{\beta}|\mathrm{B}_1^{j-1}) = \max_{\beta}(I(b[j]; \widehat{b}[j]|\mathrm{B}_1^{j-1})$ is obtained by differentiating (11) with respect to the prior probability $\beta_1 = \beta$ and put equal to zero. After some mathematical simplifications, the prior probability β_m at which mutual information is maximum can be obtained as

$$\beta_m = \frac{P_f[j|\mathrm{B}_1^{j-1}]\,(2^{\Theta} + 1) - 1}{(P_f[j|\mathrm{B}_1^{j-1}])] - P_d[j|\mathrm{B}_1^{j-1}])\,(2^{\Theta} + 1)}, \tag{12}$$

where $\Theta \triangleq \frac{H(P_d[j|\mathrm{B}_1^{j-1}]) - H(P_f[j|\mathrm{B}_1^{j-1}])}{P_d[j|\mathrm{B}_1^{j-1}] - P_f[j|\mathrm{B}_1^{j-1}]}$, and $H(a)$ denotes the binary entropy function. After putting β_m in (11) and some mathematical simplification, the closed form expression for the term $(I_m^{\beta}|\mathrm{B}_1^{j-1}) = H(q_0[j]) - (1-\beta_m)H(P_f[j|\mathrm{B}_1^{j-1}]) - \beta_m H(P_d[j|\mathrm{B}_1^{j-1}])$, where $q_0[j] \triangleq \Pr(\widehat{b}[j] = 0)$ and $q_1[j] \triangleq \Pr(\widehat{b}[j] = 1)$. The throughput of the channel is defined as the maximum of the average mutual information $\hat{I}$ about the decision threshold $\eta[j]$ and can be expressed as [21]

$$C = \max_{\eta[j]}(\widehat{I}) \text{ bits/slot}, \tag{13}$$

where average mutual information $\widehat{I}$ considering all the possible realizations is given as $\widehat{I} = \frac{1}{K} \sum_{j=1}^{K} \sum_{\mathrm{B}_1^{j-1} \in \chi} (I_m^{\beta}|\mathrm{B}_1^{j-1})/2^{j-1}$.

3) Numerical Analysis: Analysis of the anomalous diffusive channel is carried out in terms of average mutual information and average probability of error, which is shown in Fig. 2. The system parameters[4] chosen are : D_f = 5 μm^2/s, τ = 3.3 s, $Q_s \in \{100, 200, 10^3\}$, d = 10 μm, α = $[0.5 - 2]$, Δt = 0.001 s, β = 0.5, and K = 5. To calculate the number of molecules at RX, we use the CDF derived in Lemma 1. Subsequently, Monte-Carlo simulations are performed for 10^3 realizations to validate the expressions of $\overline{P}_e$ and $\hat{I}$, and it can be observed that the simulation results corroborate the analytical expressions. One can observe from Fig. 2 that for super-diffusion the average probability of error is minimal compared to the sub-diffusion and normal-diffusion phenomena. Moreover, the average mutual information is maximum in case of super-diffusion compared to the two other diffusion phenomena. Also, for the given value of α, the average probability of error achieves its minimum value and corresponding mutual information achieves its maximum value at the optimal threshold η^*. Fig. 3 shows the effect of anomalous coefficient α on the throughput C for the number of transmitted molecules $Q_s = 200$. This figure reveals that as the value of α increases, the value of C increases for any given time-slot duration. Numerically, for $\tau = 3.33$ s, we obtain $C = 0.0631$ bits/slot for $\alpha = 1$ (normal-diffusion) and $C = 0.045$ bits/slot for $\alpha = 0.5$ (sub-diffusion) and the value C increases to 0.297 bits/slot for $\alpha = 2$ (super-diffusion). Furthermore, the value of C increases

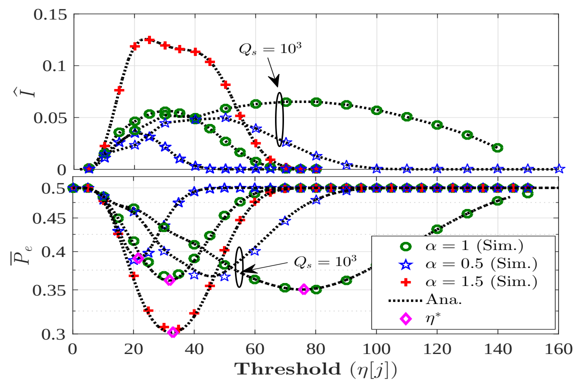

Fig. 2: Average mutual information $\widehat{I}$, and the average probability of error as a function of decision threshold η. Except where indicated, number of molecules released is $Q_s = 100$.

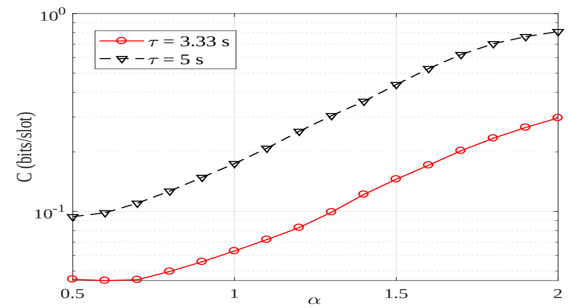

Fig. 3: Throughput (cf. (13)) as a function of anomalous coefficient α for the given value of time-slot duration τ.

[4]It is worth noting that the chosen system parameters make the Poisson approximation of the Binomial distribution more accurate than the normal approximation [22].

to $C = 0.81$ bits/slot for $\tau = 5$ s, for the case of super-diffusion.

V. Conclusion

A molecular communication system with anomalous diffusion inside a 1-D environment is considered. The expressions of FPTD, peak pulse time, and peak concentration have been derived. Furthermore, the analysis was extended to find the average probability of error and throughput for the anomalous diffusive molecular communication channel.

Appendix A
Proof of Lemma 1

Let x_o and x_a be the emitting and absorbing points for the tagged molecule. Let T be the first passage time which is defined as $T = \inf\{t : x(t) = x_a\}$. The survival probability $P_s(t)$ is defined as the probability that the tagged molecule has remained at a position $x \leq x_a$ for all times up to t, and is given by [23]

$$P_s(t) = \int_{-\infty}^{x_a} c(x, t, x_o, x_a) dx \, , \tag{14}$$

where $c(x, t, x_o, x_a)$ denotes the PDF satisfying absorbing boundary condition ($c(x_a, t) = 0$) in (3) and is given as

$$c(x, t, x_o, x_a) = \frac{1}{\sqrt{4\pi D_f t^\alpha}} \left[\exp\left(-\frac{(x-x_o)^2}{4D_f t^\alpha} \right) - \exp\left(-\frac{(x-(2x_a-x_o)^2}{4D_f t^\alpha} \right) \right]. \tag{15}$$

The survival probability $P_s(t)$ after solving (14) is obtained as $P_s(t) = \text{erf}\left(\frac{x_a - x_o}{2\sqrt{D_f t^\alpha}} \right)$. For the absorbing boundary condition, i.e., $c(x_a, t) = 0$, the FPTD can be obtained by differentiating survival probability $P_s(t)$ with respect to t as $f_p(t) = -\frac{\partial P_s(t)}{\partial t}$. Differentiating (14) with respect to the t leads to (4). For $\alpha = 1$, (4) can be simplified as

$$f_p(t) = \frac{d}{\sqrt{4\pi D_f t^3}} \exp\left(\frac{-d^2}{4D_f t} \right), \tag{16}$$

where $d \triangleq |x_a - x_o|$ denotes the Euclidean distance between molecule emtting and absorbing points. One can note that (16) is the PDF of FPTD for a normally-diffusive 1-D medium [2]. Furthermore, the corresponding cumulative density function is obtained as $F(t) = \int_0^t f_p(t^{'})\, dt^{'} = \frac{1}{\alpha}\text{erfc}\left(\frac{d}{\sqrt{4 D_f t^\alpha}} \right)$.

References

[1] T. Nakano, "Molecular communication: A 10 year retrospective," *IEEE Trans. Mol. Biol. Multi-Scale Commun.*, vol. 3, no. 2, pp. 71–78, June 2017.

[2] N. Farsad, H. B. Yilmaz, A. Eckford, C.-B. Chae, and W. Guo, "A comprehensive survey of recent advancements in molecular communication," *IEEE Commun. Surveys Tuts.*, vol. 18, no. 3, pp. 1887–1919, 2016.

[3] B. I. Henry, T. A. Langlands, and P. Straka, "An introduction to fractional diffusion," in *Complex Physical, Biophysical and Econophysical Systems*. World Scientific, 2010, pp. 37–89.

[4] Y. E. Ryabov, "Behavior of fractional diffusion at the origin," *Physical Review E*, vol. 68, no. 3, p. 030102, 2003.

[5] H.-J. Kim, "Anomalous diffusion induced by enhancement of memory," *Physical Review E*, vol. 90, no. 1, p. 012103, 2014.

[6] J.-H. Jeon, A. V. Chechkin, and R. Metzler, "Scaled brownian motion: a paradoxical process with a time dependent diffusivity for the description of anomalous diffusion," *Physical Chemistry Chemical Physics*, vol. 16, no. 30, pp. 15 811–15 817, 2014.

[7] M. Magdziarz, A. Weron, K. Burnecki, and J. Klafter, "Fractional brownian motion versus the continuous-time random walk: A simple test for subdiffusive dynamics," *Physical review letters*, vol. 103, no. 18, p. 180602, 2009.

[8] T. N. Cao, D. P. Trinh, Y. Jeong, and H. Shin, "Anomalous diffusion in molecular communication," *IEEE Commun. Lett.*, vol. 19, no. 10, pp. 1674–1677, 2015.

[9] M. U. Mahfuz, D. Makrakis, and H. T. Mouftah, "Concentration-encoded subdiffusive molecular communication: Theory, channel characteristics, and optimum signal detection," *IEEE Transactions on NanoBioscience*, vol. 15, no. 6, pp. 533–548, Sep. 2016.

[10] T. C. Mai, M. Egan, T. Q. Duong, and M. Di Renzo, "Event detection in molecular communication networks with anomalous diffusion," *IEEE Communications Letters*, vol. 21, no. 6, pp. 1249–1252, June 2017.

[11] D. P. Trinh, Y. Jeong, H. Shin, and M. Z. Win, "Molecular communication with anomalous diffusion in stochastic nanonetworks," *IEEE Trans. on Commun.*, vol. 67, no. 12, pp. 8378–8393, Dec 2019.

[12] D. P. Trinh, Y. Jeong, H. Shin, and M. Z. Win, "Molecular communication in h-diffusion," *arXiv:1911.01163*, 2019.

[13] E. S. Hui, E. Fieremans, J. H. Jensen, A. Tabesh, W. Feng, L. Bonilha, M. V. Spampinato, R. Adams, and J. A. Helpern, "Stroke assessment with diffusional kurtosis imaging," *Stroke*, vol. 43, no. 11, pp. 2968–2973, 2012.

[14] L. Chouhan, P. K. Sharma, and N. Varshney, "Optimal transmitted molecules and decision threshold for drift-induced diffusive molecular channel with mobile nanomachines," *IEEE Trans. on NanoBiosci.*, vol. 18, no. 4, pp. 651–660, Oct 2019.

[15] A. Noel, K. C. Cheung, and R. Schober, "Optimal receiver design for diffusive molecular communication with flow and additive noise," *IEEE Trans. Nanobiosci.*, vol. 13, no. 3, pp. 350–362, 2014.

[16] P. Manocha, G. Chandwani, and S. Das, "Dielectrophoretic relay assisted molecular communication for in-sequence molecule delivery," *IEEE Trans. Nanobiosci.*, vol. 15, no. 7, pp. 781–791, 2016.

[17] C. Derec, M. Smerlak, J. Servais, and J.-C. Bacri, "Anomalous diffusion in microchannel under magnetic field," *Physics Procedia*, vol. 9, pp. 109–112, 2010.

[18] A. Albinali, R. Holy, H. Sarak, and E. Ozkan, "Modeling of 1d anomalous diffusion in fractured nanoporous media," *Oil & Gas Science and Technology–Revue d$^{'}$ IFP Energies nouvelles*, vol. 71, no. 4, p. 56, 2016.

[19] I. Llatser, A. Cabellos-Aparicio, M. Pierobon, and E. Alarcón, "Detection techniques for diffusion-based molecular communication," *IEEE Jour. on Sel. Areas in Commun.*, vol. 31, no. 12, pp. 726–734, 2013.

[20] L. Lin, C. Yang, M. Ma, S. Ma, and H. Yan, "A clock synchronization method for molecular nanomachines in bionanosensor networks," *IEEE Sensors J.*, vol. 16, no. 19, pp. 7194–7203, 2016.

[21] B. Lathi and Z. Ding, *Modern Digital and Analog Communication Systems*, ser. Oxford series in electrical and computer engineering. Oxford University Press, 2018.

[22] H. B. Yilmaz and C. B. Chae, "Arrival modelling for molecular communication via diffusion," *Electronics Lett.*, vol. 50, no. 23, pp. 1667–1669, 2014.

[23] M. Ralf, R. Sidney, and O. Gleb, *First-passage phenomena and their applications*. World Scientific, 2014, vol. 35.